Fault-tolerant Quantized Control for Switched Neural Networks with Actuator Faults and Dynamic Output Quantization

Yue Su, Xinrui Wang, Weipeng Tai, Jianping Zhou

***Abstract*—This paper examines fault-tolerant quantized control for neural networks under persistent dwell-time switching, considering the presence of actuator faults and dynamic output quantization. The dynamic scaling factor (DSF) of the quantizer is designed as a piecewise function concerning the output to avoid the possibility of division by zero. To reduce conservatism, the controller is designed to combine the system model with a time scheduler constructed with a minimum time span. A sufficient condition for the asymptotic stability and $\mathcal{L}_2$-gain of the closed-loop system is derived using a piecewise Lyapunov functional and decoupling approach. When the condition is satisfied, the needed feedback gains and the parameter range associated with the DSF can be determined by exact mathematical expressions. For comparison, feedback gains that depend only on the system mode are also studied, and the corresponding design method is presented. The numerical simulation results demonstrate the effectiveness of the proposed control scheme.**

***Index Terms*—Neural network, Persistent dwell-time switching, Actuator fault, Dynamic output quantization**

I. Introduction

SWITCHED neural networks (SNNs) consist of subsystems representing neural network models and a switching rule determining which subsystem is activated [1, 2]. The switching rule in SNNs can be broadly categorized into two types: state-related and time-related. Typical time-related switching rules include dwell-time (DT) switching [3], average dwell-time (ADT) switching [4], and persistent dwell-time (PDT) switching [5]. PDT switching divides the entire timeline into different phases. Each phase comprises a non-switching portion of at least a predetermined duration and a fast-switching portion with a switching period not exceeding a specified length. In contrast to DT and ADT switching methods, PDT switching better accommodates for characterizing the dynamic behavior involving both rapid and slow switching that occurs sequentially in a switched system [6–8].

The rapid advancements in network and communication technologies have heightened the focus on the networked control of SNNs. In this context, the transmission of control signals within the networked framework faces inherent constraints posed by limited channel throughput and bandwidth, which can precipitate detrimental scenarios including data loss and communication congestion. To mitigate these issues and optimize communication efficiency, quantizing signals before transmission has emerged as a crucial step [9–11]. Guan et al. [12] designed a logarithmic quantization controller for the finite-time $\mathcal{H}_\infty$-synchronization of discrete-time SNNs. In [13], Liu et al. explored the asymptotic synchronization of Markov jumping SNNs and presented boundary quantization control strategies. In the study of $\mathcal{H}_\infty$ stabilization for delayed SNNs, Yan et al. [14] considered dynamic output quantization and presented quantized sampled-data controller designs based on two classes of two-sided loop functionals. In contrast to the static quantizers used in [12, 13], the dynamic quantizers used in [14] can effectively prevent signal saturation due to the effect of dynamic scaling factors (DSFs).

Furthermore, in practical control systems, actuator faults are frequent and often lead to a series of unpredictable and serious consequences, such as degradation of controller performance or even damage to controller components [15, 16]. To cope with this challenge, fault-tolerant control has been widely introduced into the control field in the past decades as a practical solution. Jin et al. [17] employed a neural network to estimate unknown actuator fault bounds in a fault-tolerant consensus protocol for multi-dimensional multi-agent systems. Zhang et al. [18] proposed a comprehensive neural learning-based fault-tolerant method, incorporating four adaptively tuned parameters, to accomplish path-following for underactuated vehicles, effectively addressing unknown actuator faults. In [19], Wang et al. developed fault-tolerant control strategies for synchronizing memristor-based SNNs in the presence of actuator effectiveness faults and lock-in-place faults. These studies have demonstrated that fault-tolerant control can effectively compensate for the effects of faults on the controlled system to ensure the desired performance of the controller system.

Based on the above discussion, the focus of the present work is on fault-tolerant quantized control for SNNs under PDT switching in the presence of actuator faults and dynamic output quantization. To our knowledge, there are few studies in the control designs of SNNs in the existing literature that consider both factors simultaneously, despite their potential importance. Unlike [14], the DSF is designed as a piecewise function concerning the output, which allows us to avoid the possibility of division by zero. In this paper, a criterion for the asymptotic stability and $\mathcal{L}_2$-gain of the closed-loop SNN is established by means of a piecewise Lyapunov-Krasovskii

Manuscript received May 5,2024; revised November 6,2024

Yue Su is a postgraduate student at the School of Computer Science and Technology, Anhui University of Technology, Ma'anshan 243032, China (e-mail: ysu@ahut.edu.cn).

Xinrui Wang is an undergraduate student at the School of Computer Science and Technology, Chengdu University of Technology, Chengdu 610051, China (e-mail: wang.xinrui1@student.zy.cdut.edu.cn).

Weipeng Tai is a full professor at the School of Computer Science and Technology, Anhui University of Technology, Ma'anshan 243032, China (corresponding author, e-mail: taiweipeng@ahut.edu.cn).

Jianping Zhou is a full professor at the School of Computer Science and Technology, Anhui University of Technology, Ma'anshan 243032, China (e-mail: jpzhou0@gmail.com).

functional (LKF) and some decoupling approaches. To reduce conservatism, the controller is designed to combine the system model with a time scheduler constructed with a minimum time span. The needed feedback gains and the value range of a parameter associated with the DSF can be determined by exact mathematical expressions when the criterion is met. For comparison, the feedback gains that depend only on the system mode are also studied, and the corresponding design method is proposed. Finally, the validity of the proposed control scheme is demonstrated through numerical simulation.

II. Preliminaries

Consider the SNN model with PDT switching given by

$$\begin{cases} \dot{x}(t) = A_{\delta(t)}x(t) + B_{\delta(t)}h(x(t)) + W_{\delta(t)}u^f(t) \\ \qquad + \tilde{B}_{\delta(t)}h(x(t-\nu)) + E_{\delta(t)}\epsilon(t) \\ y(t) = C_{\delta(t)}x(t) \\ z(t) = D_{\delta(t)}x(t) + G_{\delta(t)}\epsilon(t) \end{cases} \tag{1}$$

where $x(t) \in \mathbb{R}^n$, $u^f(t) \in \mathbb{R}^{n_y}$, $y(t) \in \mathbb{R}^{n_y}$, $z(t) \in \mathbb{R}^{n_z}$, and $\epsilon(t) \in \mathbb{R}^{n_w}$ are the state variable, control input with possible actuator faults, measured output, controlled output and disturbance input, respectively; $h(x(t)) = col\{h_1(x_1(t)), ..., h_n(x_n(t))\} \in \mathbb{R}^n$ stands to the activation function, where $h_i(\cdot)$ satisfies $h(0) = 0$ and the usual Lipschitz condition with coeffcient $H_i > 0$ [20, 21]; $\nu > 0$ is the time delay and $f \in \mathcal{M}$; $\delta(t)$ is the PDT switching signal that maps $[t_0, \infty)$ to $\mathcal{N}_s = \{1, 2, \ldots, s\}$ with s indicating the overall number of subsystems. The switching sequence $t_0, t_1, t_2...$, are unknown a prior but known immediately. The minimum time span between any two neighboring switching moments is denoted as $h_T = \min_{l\in\mathbb{Z}_+}(t_{l+1} - t_l)$.

The model of actuator faults can be expressed as

$$u^f(t) = M_f u(t), \tag{2}$$

where M_f is the actuator faults matrix, defined as $M_f = diag\{m_{1f}, \ldots, m_{pf}\}$ with $0 \le \widetilde{m}_{jf} \le m_{jf} \le \widehat{m}_{jf} \le 1\,(j = 1, \ldots, p)$ [22, 23]. Here $\widetilde{m}_{jf}$ and $\widehat{m}_{jf}\,(j = 1, \ldots, p)$ are known constants.

We define

$$M_{0f} = \text{diag}\left\{m_{01}^f, ..., m_{0p}^f\right\}, M_{1f} = \text{diag}\left\{m_{11}^f, ..., m_{1p}^f\right\}$$

with

$$m_{0j}^f = (\widehat{m}_{jf} + \widetilde{m}_{jf})/2,$$
$$m_{1j}^f = (\widehat{m}_{jf} - \widetilde{m}_{jf})/2\,(j = 1, ..., p).$$

Then, fault matrix M_f can be rewritten to

$$M_f = M_{0f} + M_{1f}\Lambda_f, \tag{3}$$

where

$$\Lambda_f = diag\{\lambda_{1f}, ..., \lambda_{pf}\}, -1 \le \lambda_{jf} \le 1, j = 1, ..., p.$$

Remark 1. Based on M_f, when $M_f = I$, the system actuator is normal; $M_f = 0$ indicates that the system actuator is completely failed; and $0 \le M_f < I$ indicates that the actuator is partially failed and the actuator efficiency is reduced.

Considering the limited bandwidth of the communication channel, measurement output $y(t)$ is quantized prior to transmission. The employed dynamic quantizer is formulated as

$$Q_y(y(t)) = \psi_y(t) Q\left(\frac{y(t)}{\psi_y(t)}\right), \tag{4}$$

where $\psi_y(t) > 0$ is the DSF, which, as in [24, 25], is defined as a function with respect to $y(t)$ to preclude division by zero:

$$\psi_y(t) = \begin{cases} 1, & y(t) = 0, \\ \psi\|y(t)\|, & y(t) \neq 0, \end{cases} \tag{5}$$

$\psi > 0$ is a scalar to be ascertained, and

$$Q\left(\frac{y(t)}{\psi_y(t)}\right) = col\left\{q\left(\frac{y_1(t)}{\psi_y(t)}\right), \ldots, q\left(\frac{y_{n_y}(t)}{\psi_y(t)}\right)\right\}. \tag{6}$$

In (6), $q(\cdot)$ is a static quantizer with $q(0) = 0$ and

$$\begin{aligned} |q(\vartheta(t)) - \vartheta(t)| \le \omega_q, \quad |\vartheta(t)| \le \omega_s, \\ |q(\vartheta(t)) - \vartheta(t)| > \omega_q, \quad |\vartheta(t)| > \omega_s, \end{aligned} \tag{7}$$

where $\omega_q, \omega_s \in \mathbb{R}_+$ denote the quantization error bound and quantization saturation threshold, respectively. Based on equations (4) to (7), it can be inferred that

$$\begin{aligned} \|e_y(t)\| \le \sqrt{n_y}\psi_y(t)\omega_q, \quad \|y(t) \le \psi_y(t)\omega_s\|, \\ \|e_y(t)\| > \sqrt{n_y}\psi_y(t)\omega_q, \quad \|y(t) > \psi_y(t)\omega_s\|, \end{aligned} \tag{8}$$

where

$$e_y(t) = Q(y(t)) - y(t). \tag{9}$$

The feedback controller after dynamic quantization of the output signal is

$$u(t) = \mathcal{K}_{\delta(t),r_t} Q(y(t)) \tag{10}$$

for $t \in [t_{r(s)+k}, t_{r(s)+k+1})$, where $K_{\delta(t),r_t}$ is the gain matrix. In (10), r_t as a time scheduler is defined as:

$$r_t = \begin{cases} \left\lfloor \dfrac{(t - t_{r(s)})}{h_T} \right\rfloor, & t \in [t_{r(s)}, t_{r(s)} + \varsigma), \\ b_\varsigma, & t \in [t_{r(s)} + \varsigma, t_{r(s)+1}), \\ \left\lfloor \dfrac{(t - t_\varepsilon)}{h_T} \right\rfloor, & t \in [t_{r(s)+1}, t), \end{cases} \tag{11}$$

where $b_\varsigma = \left\lfloor \frac{\varsigma}{h_T} \right\rfloor$, $t_\varepsilon \triangleq \max\left\{t_{r(s)+k} \le t, 1 \le k \le n_r\right\}$ and h_T is the minimum time span.

Substituting model of actuator faults (2) and controller (10) into (1), we can obtain the following closed-loop SNN:

$$\begin{aligned} \dot{x}(t) = & (A_{\delta(t)} + B_{\delta(t)}M_f\mathcal{K}_{\delta(t),r_t}C_{\delta(t)})x(t) \\ & + \tilde{B}_{\delta(t)}h(x(t-\nu)) + B_{\delta(t)}M_f\mathcal{K}_{\delta(t),r_t}e_y(t) \\ & + W_{\delta(t)}h(x(t)) + E_{\delta(t)}\epsilon(t). \end{aligned} \tag{12}$$

At the end of this section, let us recall two important lemmas:

Lemma 1. [26] Let $\mathcal{I}, \mathcal{F}, \mathcal{W}_a$, and $\mathcal{W}_b$ be real matrices of suitable dimensions. Then $\mathcal{I} + He(\mathcal{W}_a\mathcal{F}\mathcal{W}_b) < 0$ for $\mathcal{F}^T\mathcal{F} \le I$, if there exist only one scalar $\kappa > 0$ such that

$$\mathcal{I} + \kappa^{-1}\mathcal{W}_a\mathcal{W}_a^T + \kappa\mathcal{W}_b^T\mathcal{W}_b < 0.$$

Lemma 2. [27] Consider closed-loop SNN (12), assume that there are $\alpha > 0$, $\mu > 1$,$\gamma > 0$, and a right-continuous Lyapunov function $V_{\delta(t)}(x(t), t) \to \mathbb{R}$ such that

$$f_1(\|x(t)\|) \le V_{\delta(t)}(x(t), t) \le f_2(\|x(t)\|_v), \tag{13}$$

$$\dot{V}_{\delta}(x(t),t) \leq -\alpha V_{\delta(t)}(x(t),t) - \Gamma(s) \leq 0, \quad (14)$$

$$V_{\delta(t_k)}(x(t_k),t_k) \leq \mu \lim_{t\to t_k^-} V_{\delta(t)}(x(t),t) \quad (15)$$

for $t > t_0$ and $k \in \mathbb{Z}_+$, where f_1 and f_2 are two functions belonging to $\mathcal{F}_\infty$, and $\Gamma(s) = \|z(t)\|^2 - \gamma^2\|\epsilon(t)\|^2$. Then, for any PDT switching signal satisfies

$$\varsigma > \frac{\beta_T \ln \mu}{\alpha} - \sigma, \quad (16)$$

closed-loop SNN (12) is asymptotically stable with an $\mathcal{L}_2$-gain, which is no greater than

$$\gamma^* = \gamma\sqrt{\frac{\alpha\mu^{\beta_T}}{\alpha - \frac{\beta_T \ln \mu}{\varsigma+\sigma}}} \quad (17)$$

where $\beta_T = \frac{\sigma}{h_T} + 1$.

III. Controller design

Based on closed-loop SNN (12), we propose a method to determine the controller gains and the ψ range associated with the DSF $\psi_y(t)$.

Theorem 1. For any $i \in \mathcal{N}_d$, $j \in \mathcal{N}_\varsigma$, given $\alpha > 0$, $\mu > 0$, $\varphi_y > 0$, $\omega_s > 0$, $\iota > 0$, and $\rho > 0$, suppose there exist scalar constants $\varphi_y > 0$ and $\gamma > 0$, matrices $P_{i,j} > 0$, $Q > 0$, $S_{i,j}$, $U_{i,j}$, and diagonal matrix $R > 0$ such that

$$\begin{bmatrix} \Gamma_{1,i,j}^{11} & \Gamma_{1,i,j}^{12} & \Gamma_{1,i,j}^{13} & \Gamma_{1,i,j}^{14} & \Gamma_i^{15} & \Gamma_{1,i,j}^{16} & \Gamma_{1,i,j}^{17} \\ * & \Gamma_i^{22} & 0 & 0 & 0 & 0 & 0 \\ * & * & \Gamma_i^{33} & 0 & 0 & 0 & 0 \\ * & * & * & \Gamma_i^{44} & 0 & 0 & 0 \\ * & * & * & * & -I & \Gamma_i^{56} & 0 \\ * & * & * & * & * & \Gamma_{i,j}^{66} & 0 \\ * & * & * & * & * & * & -\mu I \end{bmatrix} < 0, \quad (18)$$

$$\begin{bmatrix} \Gamma_{2,i,j}^{11} & \Gamma_{2,j}^{12} & \Gamma_{2,i,j}^{13} & \Gamma_{2,i,j}^{14} & \Gamma_i^{15} & \Gamma_{2,i,j}^{16} & \Gamma_{2,i,j}^{17} \\ * & \Gamma_i^{22} & 0 & 0 & 0 & 0 & 0 \\ * & * & \Gamma_i^{33} & 0 & 0 & 0 & 0 \\ * & * & * & \Gamma_i^{44} & 0 & 0 & 0 \\ * & * & * & * & -I & \Gamma_i^{56} & 0 \\ * & * & * & * & * & \Gamma_{i,j}^{66} & 0 \\ * & * & * & * & * & * & -\mu I \end{bmatrix} < 0, \quad (19)$$

hold for any $j \in \mathcal{N}_\varsigma - b_\varsigma$, and

$$\begin{bmatrix} \Gamma_{3,i,j}^{11} & \Gamma_{3,i,j}^{12} & \Gamma_{3,i,j}^{13} & \Gamma_{3,i,j}^{14} & \Gamma_i^{15} & \Gamma_{3,i,j}^{16} & \Gamma_{3,i,j}^{17} \\ * & \Gamma_i^{22} & 0 & 0 & 0 & 0 & 0 \\ * & * & \Gamma_i^{33} & 0 & 0 & 0 & 0 \\ * & * & * & \Gamma_i^{44} & 0 & 0 & 0 \\ * & * & * & * & -I & \Gamma_i^{56} & 0 \\ * & * & * & * & * & \Gamma_{i,j}^{66} & 0 \\ * & * & * & * & * & * & -\mu I \end{bmatrix} < 0, \quad (20)$$

$$P_{i,0} \leq \mu P_{l,j}, \quad (21)$$

$$1/\omega_s < \sqrt{\varphi_y} \quad (22)$$

hold for any $l \in \mathcal{N}_d - \{i\}$ and $j \in \mathcal{N}_\varsigma - \{0\}$, where

$$\begin{aligned}
\Gamma_{1,i,j}^{11} &= \alpha P_{i,j} + He(P_{i,j}A_i + W_i M_{0i} U_{i,j})C_i \\
&\quad + (P_{i,j+1} - P_{i,j})/h_T + D_i^T D_i + HQH + \iota C_i^T C_i, \\
\Gamma_{2,i,j}^{11} &= \alpha P_{i,j+1} + He(P_{i,j+1}A_i + W_i M_{0i} U_{i,j}) \\
&\quad + (P_{i,j+1} - P_{i,j})/h_T + D_i^T D_i + HQH + \iota C_i^T C_i, \\
\Gamma_{3,i,j}^{11} &= \alpha P_{i,j} + He(P_{i,j}A_i + W_i M_{0i} U_{i,j}) \\
&\quad + D_i^T D_i + HQH + \iota C_i^T C_i, \\
\Gamma_{1,i,j}^{12} &= \Gamma_{3,i,j}^{12} = P_{i,j}B_i,\ \Gamma_{2,i,j}^{12} = P_{i,j+1}B_i, \\
\Gamma_{1,i,j}^{13} &= \Gamma_{3,i,j}^{13} = P_{i,j}\tilde{B}_i,\ \Gamma_{2,i,j}^{13} = P_{i,j+1}\tilde{B}_i, \\
\Gamma_{1,i,j}^{14} &= \Gamma_{3,i,j}^{14} = P_{i,j}E_i + D_i^T G_i, \\
\Gamma_{2,i,j}^{14} &= P_{i,j+1}E_i + D_i^T G_i, \\
\Gamma_{1,i,j}^{16} &= \Gamma_{3,i,j}^{16} = P_{i,j}W_i M_{0i} - W_i M_{0i} S_{i,j} + \rho(U_{i,j}C_i)^T, \\
\Gamma_{2,i,j}^{16} &= P_{i,j+1}W_i M_{0i} - W_i M_{0i} S_{i,j} + \rho(U_{i,j})^T, \\
\Gamma_{1,i,j}^{17} &= \Gamma_{3,i,j}^{17} = P_{i,j}W_i M_{1i}, \Gamma_{2,i,j}^{17} = P_{i,j+1}W_i M_{1i}, \\
\Gamma_i^{15} &= W_i M_{0i} U_{i,j},\ \Gamma_i^{22} = L - Q,\ \Gamma_i^{33} = -e^{-\alpha\nu}L, \\
\Gamma_i^{44} &= G_i^T G_i - \gamma^2 I,\ \Gamma_i^{56} = \rho U_{i,j}^T, \\
\Gamma_{i,j}^{66} &= -\rho(S_{i,j} + S_{i,j}^T) + \mu I, \\
H &= diag\{H_1, H_2, \ldots, H_n\}.
\end{aligned}$$

Then, for any PDT ς satisfying (16), the closed-loop SNN is asymptotically stable with $\mathcal{L}_2$-gain no greater than γ^* given in (17). Furthermore, the feedback gains and the parameter ψ range associated with the DSF $\psi_y(t)$ for the required dynamic quantization controller can be designed as

$$\mathcal{K}_{i,j} = S_{i,j}^{-1} U_{i,j},\ i \in \mathcal{N}_d,\ j \in \mathcal{N}_\varsigma, \quad (23)$$

$$\sqrt{\varphi_y} \leq \psi \leq 2\sqrt{\varphi_y}, \quad (24)$$

respectively.

Proof: Define $\zeta_j = jh_T$, $j \in \mathcal{N}_\varsigma$. From (11), we establish the following intervals:

$$\begin{aligned}
[t_{r(s)}, t_{r(s)+1}) &= \cup_{j=0}^{b_\varsigma - 1} [t_{r(s)+\zeta_j}, t_{r(s)+\zeta_{j+1}}) \\
&\quad \cup [t_{r(s)+\zeta_{b_\varsigma}}, t_{r(s)+1}), \\
[t_{r(s)+1}, t_{r(s+1)}) &= \cup_{k=1}^{n_r} [t_{r(s)+k}, t_{r(s)+1}), \\
[t_{r(s)+k}, t_{r(s)+k+1}) &= \cup_{j=0}^{b_{r,k}-1} [t_{r(s)+k+\zeta_j}, t_{r(s)+k+\zeta_{j+1}}) \\
&\quad \cup [t_{r(s)+k+\zeta_{b_{r,k}}}, t_{r(s)+k+1}).
\end{aligned}$$

We have $1 \leq b_{r,k} = \left\lfloor \frac{\sigma_{r,k}}{h_T} \right\rfloor < b_\varsigma$, in which $\sigma_{r,k}$ denotes the interval $[t_{r(s)}, t_{r(s)+1})$. Therefore, according to the PDT switching rule, $\sigma_{r,k} < \varsigma$ is true.

From the intervals above, we build a piecewise LKF accordingly:

$$V_{\delta(t)}(x(t),t) = V_0(t) + \begin{cases} V_{1,\delta(t)}(x(t),t), & t \in [t_{r(s)} + \zeta_j, t_{r(s)+\zeta_{j+1}}) \\ & j = 0, 1, \ldots, b_\varsigma - 1, \\ V_{2,\delta(t)}(x(t),t), & t \in [t_{r(s)} + \zeta_{b_\varsigma}, t_{r(s)+1}), \\ V_{3,\delta(t)}(x(t),t), & t \in [t_{r(s)+k} + \zeta_j, t_{r(s)+k} + \zeta_{j+1}) \\ & j = 0, 1, \ldots, b_{r,k} - 1, \\ V_{4,\delta(t)}(x(t),t), & t \in [t_{r(s)+k} + \zeta_{b_{r,k}}, t_{r(s)+k+1}), \end{cases} \quad (25)$$

here $1 < k < n_r, r \in \mathbb{Z}_+$, and

$$V_0(t) = \int_{t-\nu}^{t} e^{\alpha(s-t)} h^T(x(s)) L h(x(s))\, ds,$$

$$\begin{aligned}
V_{1,\delta(t)}(x(t),t) &= x^T(t)[(1-\varrho_{1t})P_{\delta(t),j} + \varrho_{1t}P_{\delta(t),j+1}]x(t), \\
V_{2,\delta(t)}(x(t),t) &= x^T(t)P_{\delta(t),b_\varsigma}x(t), \\
V_{3,\delta(t)}(x(t),t) &= x^T(t)[(1-\varrho_{2t})P_{\delta(t),j} + \varrho_{2t}P_{\delta(t),j+1}]x(t), \\
V_{4,\delta(t)}(x(t),t) &= x^T(t)P_{\delta(t),b_{r,k}}x(t)
\end{aligned}$$

with

$$\varrho_{1t}=\frac{t-(t_{r(s)}+b_j)}{h_T},\varrho_{2t}=\frac{t-(t_{r(s)+k}+b_j)}{h_T}.$$

It is evident that the aforementioned LKF $V_{\delta(t)}(x(t),t)$ exhibits right-continuous differentiability, with the exception of the switching instances. Consequently, it is enough to show that the inequality presented in (13)-(15) holds, leveraging the premise outlined in Lemma 2. Considering

$$h^T(x(s))Lh(x(s))\leq\lambda_M(L)tr(H^2)\|x(s)\|^2,$$
$$\lambda_{\delta(t),N}(\overline{P})=\max_{j\in\mathcal{N}_\varsigma}\lambda_N(P_{\delta(t),j}),$$
$$\lambda_{\delta(t),n}(\overline{P})=\min_{j\in\mathcal{N}_\varsigma}\lambda_n(P_{\delta(t),j}),$$

we have

$$\begin{aligned}&\lambda_{\delta(t),n}(\overline{P})\|x(t)\|^2\\&\leq V_{\delta(t)}(x(t),t)\leq[\lambda_{\delta(t),N}+\nu\lambda_N(L)tr(H^2)]\|x(t)\|_\nu^2,\end{aligned}$$

which implies the validity of (13).

Based on (7) and DSF, we can infer that

$$\sqrt{\varphi_y}\|y(t)\|\leq\psi_y(t)\leq2\sqrt{\varphi_y}\|y(t)\|,\tag{26}$$

from (7) and (26), we can obtain

$$\|y(t)\|\leq\sqrt{n_y}\omega_s\psi_y(t),\tag{27}$$
$$\|e_y(t)\|\leq\sqrt{n_y}\psi_y(t)\omega_q,\tag{28}$$

utilizing the expressions (26)-(28), we have

$$\|e_y(t)\|=2\sqrt{n_y}\sqrt{\varphi_y}\omega_q\|y(t)\|.\tag{29}$$

To prove (14), define the following

$$\varTheta(t)=col\left\{x(t),h(x(t)),h(x(t-\nu)),\epsilon(t),e_y(t)\right\}$$

and according to closed-loop SNN (12), we konw that

$$x^T(t)HQHx(t)>h^T(x(t))Qh(x(t)).\tag{30}$$

Furthermore, in according with (12) and (29), the following inequality can be inferred:

$$x^T(t)4n_y\varphi_y\omega_q^2C_i^TC_ix(t)-e_y^T(t)e_y(t)\geq0,$$

assume $\iota=2\sqrt{n_y}\sqrt{\varphi_y}\omega_q$.

Following the discussion in [27], we consider the following four cases:

Case 1: $t\in[t_{r(s)}+\zeta_j,t_{r(s)}+\zeta_{j+1})$, $j=0,1,\ldots,b_\varsigma-1$.

Given this case, we have

$$\begin{aligned}&\dot{V}_{\delta(t)=i}(x(t),t)\\&=h^T(x(t))Lh(x(t))-e^{-\alpha\nu}h^T(x(t-\nu))Lh(x(t-\nu))\\&\quad-\alpha V_0(t)+2x^T(t)[(1-\varrho_{1t})P_{i,j}+\varrho_{1t}P_{i,j+1}][(A_i\\&\quad+W_iM_i\mathcal{K}_{i,j}C_{i,j})x(t)+B_ih(x(t))+\tilde{B}_ih(x(t-\nu))+\\&\quad+E_i\epsilon(t)+W_iM_i\mathcal{K}_{i,j}e_y(t)]+\frac{1}{h_T}x^T(x)[P_{i,j+1}\\&\quad-P_{i,j}]x(t),\end{aligned}$$

and, thus, we can write that

$$\begin{aligned}&\dot{V}_{\delta(t)=i}(x(t),t)+\alpha V_{\delta(t)=i}(x(t),t)+\varGamma(s)\\&\leq h^T(x(t))Lh(x(t))-e^{-\alpha\nu}h^T(x(t-\nu))Lh(x(t-\nu))\\&\quad+\alpha x^T(t)[(1-\varrho_{1t})P_{i,j}+\varrho_{1t}P_{i,j+1}]x(t)\\&\quad+2x^T(t)[(1-\varrho_{1t})P_{i,j}+\varrho_{1t}P_{i,j+1}]\\&\quad\times[(A_i+W_iM_i\mathcal{K}_{i,j}C_{i,j})x(t)+B_ih(x(t))+\tilde{B}_ih(x(t-\nu))\\&\quad+E_i\epsilon(t)+W_iM_i\mathcal{K}_{i,j}e_y(t)]+\varGamma(s)\\&\quad+\frac{1}{h_T}x^T(t)(P_{i,j+1}-P_{i,j})x(t)+x^T(t)\iota^2C_i^TC_ix(t)\\&\quad-e_y^T(t)e_y(t)+x^T(t)HQHx(t)-h^T(x(t))Qh(x(t))\\&\leq(1-\varrho_{1t})\varTheta^T(t)\Pi_{1,i,j}\varTheta(t)+\varrho_{1t}\varTheta^T(t)\Pi_{2,i,j}\varTheta(t),\end{aligned}$$

in which

$$\Pi_{1,i,j}=\begin{bmatrix}\Xi_{1,i,j}^{11}&P_{i,j}B_i&P_{i,j}\tilde{B}_i&\Gamma_{1,i,j}^{14}&\Xi_{1,i,j}^{15}\\ *&L-Q&0&0&0\\ *&*&-e^{-\alpha\nu}L&0&0\\ *&*&*&\Gamma_i^{44}&0\\ *&*&*&*&-I\end{bmatrix},$$

$$\Pi_{2,i,j}=\begin{bmatrix}\Xi_{2,i,j}^{11}&P_{i,j+1}B_i&P_{i,j+1}\tilde{B}_i&\Gamma_{2,i,j}^{14}&\Xi_{2,i,j}^{15}\\ *&L-Q&0&0&0\\ *&*&-e^{-\alpha\nu}L&0&0\\ *&*&*&\Gamma_i^{44}&0\\ *&*&*&*&-I\end{bmatrix},$$

$$\begin{aligned}\Xi_{1,i,j}^{11}&=\alpha P_{i,j}+He(P_{i,j}A_i+P_{i,j}W_iM_i\mathcal{K}_{i,j}C_i)\\&\quad+D_i^TD_i+HQH+\frac{1}{h_T}[P_{i,j+1}-P_{i,j}]+\iota C_i^TC_i,\\ \Xi_{2,i,j}^{11}&=\alpha P_{i,j+1}+He(P_{i,j+1}A_i+P_{i,j+1}W_iM_i\mathcal{K}_{i,j}C_i)\\&\quad+D_i^TD_i+HQH+\frac{1}{h_T}[P_{i,j+1}-P_{i,j}]+\iota C_i^TC_i,\\ \Xi_{1,i,j}^{15}&=P_{i,j}W_iM_i\mathcal{K}_{i,j},\\ \Xi_{2,i,j}^{15}&=P_{i,j+1}W_iM_i\mathcal{K}_{i,j}.\end{aligned}$$

Case 2: $t\in[t_{r(s)}+\zeta_{b_\varsigma},t_{r(s)+1})$.

Given this case, we have

$$\begin{aligned}&\dot{V}_{\delta(t)=i}(x(t),t)+\alpha V_{\delta(t)=i}(x(t),t)+\varGamma(s)\\&\leq\varTheta^T(t)\Pi_{i,b_\varsigma}\varTheta(t),\end{aligned}$$

where

$$\Pi_{i,b_\varsigma}=\begin{bmatrix}\Xi_{i,b_\varsigma}^{11}&P_{i,b_\varsigma}B_i&P_{i,b_\varsigma}\tilde{B}_i&\Gamma_{1,i,j}^{14}&\Xi_{1,i,j}^{15}\\ *&L-Q&0&0&0\\ *&*&-e^{-\alpha\nu}L&0&0\\ *&*&*&\Gamma_i^{44}&0\\ *&*&*&*&-I\end{bmatrix},$$

$$\begin{aligned}\Xi_{i,b_\varsigma}^{11}&=\alpha P_{i,b_\varsigma}+He(P_{i,b_\varsigma}A_i+P_{i,b_\varsigma}W_iM_i\mathcal{K}_{i,b_\varsigma})+\iota C_i^TC_i\\&\quad+D_i^TD_i+HQH,\\ \Xi_{3,i,j}^{15}&=P_{i,b_\varsigma}W_iM_i\mathcal{K}_{i,b_\varsigma}.\end{aligned}$$

Case 3: $t\in[t_{r(s)+k}+\zeta_j,t_{r(s)+k}+\zeta_{j+1})$, $j=1,\ldots,b_{r,k}-1$, $k=1,2,\ldots,n_r$.

Given this case, we have

$$\begin{aligned}&\dot{V}_{\delta(t)=i}(x(t),t)+\alpha V_{\delta(t)=i}(x(t),t)+\varGamma(s)\\&\leq(1-\varrho_{2t})\varTheta^T(t)\Pi_{1,i,j}\varTheta(t)+\varrho_{2t}\varTheta^T(t)\Pi_{2,i,j}\varTheta(t),\end{aligned}$$

$\Pi_{1,i,j}$ and $\Pi_{2,i,j}$ are the same as in Case 1.

Case 4: $t\in[t_{r(s)+k}+\zeta_{b_{r,k}},t_{r(s)+k+1}]$, $k=1,2,\ldots,n_r$.

Given this case, we have

$$\begin{aligned}&\dot{V}_{\delta(t)=i}(x(t),t)+\alpha V_{\delta(t)=i}(x(t),t)+\varGamma(s)\\&\leq\varTheta^T(t)\Pi_{i,b_{r,k}}\varTheta(t),\end{aligned}$$

where

$$\Pi_{i,b_{r,k}}=\begin{bmatrix} \Xi^{11}_{i,b_{r,k}} & P_{i,b_{r,k}}B_i & P_{i,b_{r,k}}\tilde{B}_i & \Gamma^{14}_{3,i,b_{r,k}} & \Xi^{15}_{3,i,b_{r,k}} \\ * & L-Q & 0 & 0 & 0 \\ * & * & -e^{-\alpha\nu}L & 0 & 0 \\ * & * & * & \Gamma^{44}_i & 0 \\ * & * & * & * & -I \end{bmatrix},$$

$$\Xi^{11}_{i,b_{r,k}} = \alpha P_{i,b_{r,k}} + He(P_{i,b_{r,k}}A_i + P_{i,b_{r,k}}W_iM_i\mathcal{K}_{i,b_{r,k}}) + D_i^TD_i + HQH + \iota C_i^TC_i,$$

$$\Xi^{15}_{3,i,b_{r,k}} = P_{i,b_{r,k}}W_iM_i\mathcal{K}_{i,b_{r,k}}.$$

From the above analysis, it can be proven that (14) is correct when the following inequality is true:

$$\Pi_{1,i,j} < 0, 0 \le j \le b_\varsigma - 1, \quad (31)$$

$$\Pi_{2,i,j} < 0, 0 \le j \le b_\varsigma - 1, \quad (32)$$

$$\Pi_{i,j} < 0, 0 \le j \le b_\varsigma. \quad (33)$$

In addition, in the light of (23), one can write

$$\begin{aligned} &He(P_{i,j}W_iM_i\mathcal{K}_{i,j}) \\ =&He(W_iM_{0i}U_{i,j} + (P_{i,j}W_iM_i - W_iM_{0i}S_{i,j})S^{-1}_{i,j}U_{i,j}). \end{aligned} \quad (34)$$

By (34), it is obvious that (31) can be rewritten as

$$\begin{bmatrix} \Gamma^{11}_{1,i,j} & P_{i,j}B_i & P_{i,j}\tilde{B}_i & \Gamma^{14}_{1,i,j} & \Gamma^{15}_{1,i,j} \\ * & L-Q & 0 & 0 & 0 \\ * & * & -e^{-\alpha\nu}L & 0 & 0 \\ * & * & * & \Gamma^{44}_i & 0 \\ * & * & * & * & -I \end{bmatrix} + He(\Pi^A_{i,j}X^{-1}_{i,j}\Pi^B_{i,j}) < 0, \quad (35)$$

where

$$\Pi^A_{i,j} = [\ (P_{i,j}W_iM_i - W_iM_{0i}S_{i,j})^T\ 0\ 0\ 0\ 0\ ]^T,$$

$$\Pi^B_{i,j} = [\ U_{i,j}C_i\ 0\ 0\ 0\ U_{i,j}\ ].$$

Then according to the projection theorem and Schur's complement, (35) is ensured by

$$\begin{bmatrix} \Gamma^{11}_{1,i,j} & P_{i,j}B_i & P_{i,j}\tilde{B}_i & \Gamma^{14}_{1,i,j} & \Gamma^{15}_i & \Xi^{16}_{1,i,j} \\ * & L-Q & 0 & 0 & 0 & 0 \\ * & * & -e^{-\alpha\nu}L & 0 & 0 & 0 \\ * & * & * & \Gamma^{44}_i & \rho U^T_{i,j} & 0 \\ * & * & * & * & -I & 0 \\ * & * & * & * & * & \Gamma^{66}_{1,i,j} \end{bmatrix}, \quad (36)$$

where

$$\Xi^{16}_{1,i,j} = P_{i,j}W_iM_i - W_iM_{0i}S_{i,j} + \rho U^T_{i,j},$$

$$\Gamma^{66}_{1,i,j} = \rho He(S_{i,j}).$$

According to (3) and lemma 1, (36) can be re-expressed as

$$\Phi_{1,i,j} + He(\mathcal{W}_{a,i,j}\Lambda_{i,j}\mathcal{W}_{b,i,j}) < 0, \quad (37)$$

where

$$\mathit{\Pi}_{1,i,j}=\begin{bmatrix} \Gamma^{11}_{1,i,j} & P_{i,j}B_i & P_{i,j}\tilde{B}_i & \Gamma^{14}_{1,i,j} & \Gamma^{15}_i & \Gamma^{16}_{1,i,j} \\ * & L-Q & 0 & 0 & 0 & 0 \\ * & * & -e^{-\alpha\nu}L & 0 & 0 & 0 \\ * & * & * & \Gamma^{44}_i & \rho U^T_{i,j} & 0 \\ * & * & * & * & -I & 0 \\ * & * & * & * & * & \Gamma^{66}_{1,i,j} \end{bmatrix},$$

$$\mathcal{W}_{a,i,j} = [\ (P_{i,j}W_iM_{1i})^T\ 0\ 0\ 0\ 0\ 0\ ]^T,$$

$$\mathcal{W}_{b,i,j} = [\ 0\ 0\ 0\ 0\ 0\ I\ ].$$

By Schur's complement, (37) can be rewritten as (18). Using the same reasoning, it can be inferred that (32) and (33) are obtained from (19) and (20), respectively.

Finally, we demonstrate the effectiveness of (15) based on piecewise LKF (25) and (21). There are different derivation processes for different switching states as follows:

Situation $\mathcal{A}$: Slow-to-Fast Switching.

When switching at time $t_{r(s)+1}$, assuming $t_{r(s)+1} = t_f, f \in \mathbb{Z}_+$, we have

$$\begin{aligned} V_{t_f}(x(t_f), t_f) &= V_0(t_f) + V_{3,\delta(t_f)}(x(t_f), t_f) \\ &= V_0(t_f) + x^T(t)P_{\delta(t_f),0}x(t), \\ \lim_{t\to t^-_{t_f}} V_{\delta(t)}(x(t), t) &= \lim_{t\to t^-_{t_f}} [V_0(t) + V_{2,\delta(t)}(x(t), t)] \\ &= V_0(t_f) + x^T(t)P_{\delta(t_{r(s)}, b_\varsigma)}x(t). \end{aligned}$$

Situation $\mathcal{B}$: Rapid Switching.

When switching at time $t_{r(s)+k}$, assuming $t_{r(s)+k} = t_j, j \in \mathbb{Z}_+$, we have

$$\begin{aligned} V_{t_j}(x(t_j), t_j) &= V_0(t_j) + V_{3,\delta(t_j)}(x(t_j), t_j) \\ &= V_0(t_j) + x^T(t)P_{\delta(t_j),0}x(t), \\ \lim_{t\to t^-_{t_j}} V_{\delta(t)}(x(t), t) &= \lim_{t\to t^-_{t_j}} [V_0(t) + V_{4,\delta(t)}(x(t), t)] \\ &= V_0(t_j) + x^T(t)P_{\delta(t_{j-1}, b_{r,k-1})}x(t). \end{aligned}$$

Situation $\mathcal{C}$: Fast-to-Slow Switching.

When switching at time $t_{r(s)+n_r+1} = t_{r(s+1)}$, assuming $t_{r(s+1)} = t_l, l \in \mathbb{Z}_+$, we have

$$\begin{aligned} V_{t_l}(x(t_l), t_l) &= V_0(t_l) + V_{1,\delta(t_l)}(x(t_l), t_l) \\ &= V_0(t_l) + x^T(t)P_{\delta(t_l),0}x(t), \\ \lim_{t\to t^-_{t_l}} V_{\delta(t)}(x(t), t) &= \lim_{t\to t^-_{t_l}} [V_0(t) + V_{4,\delta(t)}(x(t), t)] \\ &= V_0(t_l) + x^T(t)P_{\delta(t_{l-1}, b_{r,n_r})}x(t). \end{aligned}$$

Based on the above three scenarios, for all $k \in \{1, 2, \dots, n_r + 1\}$:

$$\begin{aligned} &V_{\delta(t_{r(s)+k})}(x(t_{r(s)+k}), t_{r(s)+k}) \\ \le&\mu \lim_{t\to t^-_{r(s)+k}} V_{\delta(t)}(x(t), t), k \in 1, 2, \dots, n_r + 1, \end{aligned}$$

which implies (15). Thus, the proof is finished. ■

Remark 2. The coupling of the Lyapunov matrices with the actuator fault uncertainty directly leads to the emergence of high-order nonlinearities when designing the required dynamic quantized controller. The handling of such high-order nonlinearities is quite challenging. To address this problem, Theorem 1 proposes a method that converts the solution process of the required gain range and related parameters ψ of the DSF $\psi_y(t)$ into the solution of a series of linear matrix inequalities (LMIs). These LMIs can be easily solved and verified by the computational software MATLAB.

In Theorem 1, the controller is contingent upon both the system model and a time scheduler constructed with a minimum time span. Furthermore, when the feedback gains depend only on the system mode, as in [28–30], the form of the controller is changed to

$$u(t) = \mathcal{K}_{\delta(t)}Q(y(t)),$$

On this basis, LKF can be set to

$$V_{\delta(t)}(x(t),t) = x^T(t)P_{\delta(t)}x(t) + \int_{t-\nu}^{t} e^{\alpha(s-t)}h^T(x(s))Lh(x(s))\,ds.$$

The following corollary can be established:

Corollary 1. For any $i \in \mathcal{N}_d$, given $\alpha > 0$, $\mu > 0$, $\varphi_y > 0$, $\omega_s > 0$, $\iota > 0$, and $\rho > 0$, suppose there exist scalar constants $\varphi_y > 0$ and $\gamma > 0$, matrices $P_i > 0$, $Q > 0$, S_i, U_i, and diagonal matrix $R > 0$ satisfies

$$\begin{bmatrix} \Gamma_i^{11} & \Gamma_i^{12} & \Gamma_i^{13} & \Gamma_i^{14} & \Gamma_i^{15} & \Gamma_i^{16} & \Gamma_i^{17} \\ * & \Gamma_i^{22} & 0 & 0 & 0 & 0 & 0 \\ * & * & \Gamma_i^{33} & 0 & 0 & 0 & 0 \\ * & * & * & \Gamma_i^{44} & 0 & 0 & 0 \\ * & * & * & * & -I & \Gamma_i^{56} & 0 \\ * & * & * & * & * & \Gamma_i^{66} & 0 \\ * & * & * & * & * & * & -\mu I \end{bmatrix} < 0, \quad (38)$$

$$P_i \leq \mu P_l, \quad (39)$$

$$1/\omega_s \leq \sqrt{\varphi_y} \quad (40)$$

hold for any $l \in \mathcal{N}_d - \{i\}$, where

$$\begin{aligned} \Gamma_i^{11} &= \alpha P_i + He(P_iA_i + W_iM_{0i}U_{i,j})C_i \\ &\quad + D_i^TD_i + HQH + \iota C_i^TC_i, \\ \Gamma_i^{12} &= P_iB_i, \Gamma_i^{13} = P_i\tilde{B}_i, \\ \Gamma_i^{14} &= P_iE_i + D_i^TG_i, \Gamma_i^{15} = W_iM_{0i}U_{i,j}, \\ \Gamma_i^{16} &= P_iW_iM_{0i} - W_iM_{0i}S_i + \rho(U_i)^T, \\ \Gamma_i^{17} &= P_iW_iM_{1i}, \Gamma_i^{22} = L - Q, \\ \Gamma_i^{33} &= -e^{-\alpha\nu}L, \ \Gamma_i^{44} = G_i^TG_i - \gamma^2 I, \\ \Gamma_i^{56} &= \rho U_i^T, \Gamma_i^{66} = -\rho(S_i + S_i^T) + \mu I, \\ H &= diag\{H_1, H_2, \ldots, H_n\}. \end{aligned}$$

Then, for any PDT ς satisfying (16), the closed-loop SNN is asymptotically stable with $\mathcal{L}_2$-gain no greater than γ^* given in (17). Furthermore, the feedback gains and the value range of parameter ψ associated with DSF $\psi_y(t)$ of the needed dynamic quantization controller can be designed as

$$\mathcal{K}_i = S_i^{-1}U_i, i \in \mathcal{N}_d, j \in \mathcal{N}_\varsigma,$$
$$\sqrt{\psi_y} \leq \psi \leq 2\sqrt{\psi_y},$$

respectively.

IV. Numerical Examples

Consider SNN (1) with some parameters borrowed from [31]:

$$A_1 = \begin{bmatrix} -1 & 0 \\ 0 & -1 \end{bmatrix}, W_1 = \begin{bmatrix} -2 & 1 \\ 0 & -2 \end{bmatrix},$$

$$A_2 = \begin{bmatrix} -1 & 0 \\ 0 & -1 \end{bmatrix}, W_2 = \begin{bmatrix} -2 & 0.1 \\ 0 & -2 \end{bmatrix},$$

$$B_1 = \begin{bmatrix} -2 & -0.1 \\ -5 & 4.5 \end{bmatrix}, \tilde{B}_1 = \begin{bmatrix} -1.5 & -0.1 \\ -0.2 & -3 \end{bmatrix},$$

$$B_2 = \begin{bmatrix} 2 & -0.1 \\ -5 & 4.5 \end{bmatrix}, \tilde{B}_2 = \begin{bmatrix} -1.5 & -0.1 \\ -0.2 & -2.5 \end{bmatrix},$$

$$C_1 = C_2 = \begin{bmatrix} -1 & 0 \\ 0 & 1 \end{bmatrix}, E_1 = \begin{bmatrix} 1 \\ 2 \end{bmatrix}, E_2 = \begin{bmatrix} 0.12 \\ 0.1 \end{bmatrix},$$

TABLE I
γ^* VALUES FOR DIFFERENT ν SETTINGS

γ^*	ν				
	1.00	1.50	2.00	2.50	3.00
Theorem 1	0.7930	0.7932	0.7934	0.7936	0.7939
Corollary 1	0.7939	0.7940	0.7943	0.7945	0.7948

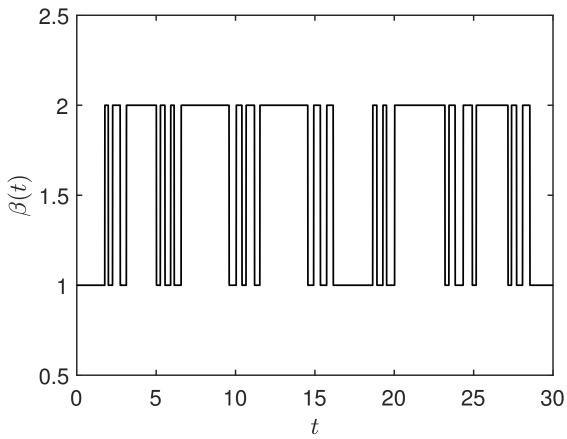

Fig. 1. Switching signal $\delta(t)$.

$$D_1 = \begin{bmatrix} 0.1 \\ -0.1 \end{bmatrix}^T, D_2 = \begin{bmatrix} 0.6 \\ -0.1 \end{bmatrix}^T, G_2 = G_1 = 0.1,$$

$$h(x(\cdot)) = \begin{bmatrix} tanh(x_1(\cdot)) \\ tanh(x_2(\cdot)) \end{bmatrix}, \epsilon(t) = 3.4e^{-0.25t}sin(2.5\pi t).$$

Besides, we assign $H_1 = H_2 = 1$, $\varsigma = 0.9$, $\sigma = 3$, and $h_T = 0.2$, and specify the parameter values $\alpha = 0.3$, $\rho = 0.1$, $\mu = 1.1$. When $\widehat{m}_{ji} = 1$, $\widetilde{m}_{ji} = 0.2\,(i,j = 1,2)$, it solves the matrix inequality in (3).

Generally speaking, the smaller the $\mathcal{L}_2$-gain, the better the anti-interference performance. Table I delineates the minimum allowable $\mathcal{L}_2$-gain corresponding to various time delay settings ν. It can be seen that as the time delay increases, the interference suppression performance decreases. Furthermore, the value of γ^* derived from Theorem 1 is always better than Corollary 1, which means that the controller design with dual dependence on mode and scheduler is better than the method that only depends on mode.

In the following, we set $\nu = 1$. The static quantizer is chosen as

$$Q(\psi(t)) = \begin{cases} \psi(t) + \omega_q sin(\psi(t)), & |\psi(t)| \leq \omega_s, \\ \psi(t) + sign(\psi(t)), & |\psi(t)| > \omega_s. \end{cases}$$

We set quantization error bound $\omega_q = 0.01$, quantization saturation threshold $\omega_s = 30$. By employing Lemma 2, we can get the parameter $\varphi_y = 0.0011$ and the feedback gains:

$$\mathcal{K}_{1,0} = \begin{bmatrix} 22.5099 & 1.7468 \\ -9.8223 & 18.4985 \end{bmatrix},$$

$$\mathcal{K}_{1,1} = \begin{bmatrix} 20.1494 & 4.7567 \\ -10.0982 & 20.0629 \end{bmatrix},$$

$$\mathcal{K}_{1,2} = \begin{bmatrix} 20.1218 & 4.8122 \\ -10.1416 & 20.1153 \end{bmatrix},$$

$$\mathcal{K}_{1,3} = \begin{bmatrix} 20.1473 & 4.8075 \\ -10.1269 & 20.1045 \end{bmatrix},$$

$$\mathcal{K}_{1,4} = \begin{bmatrix} 20.1627 & 4.8071 \\ -10.1182 & 20.1012 \end{bmatrix},$$

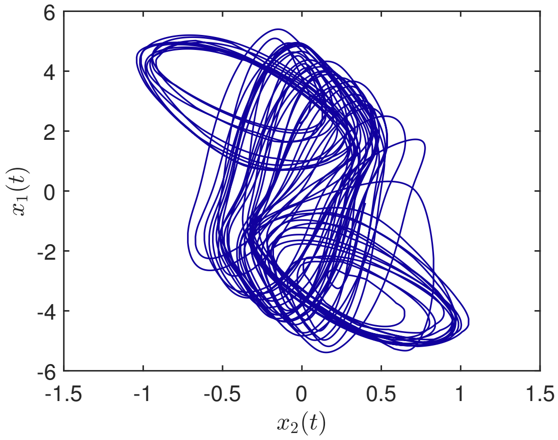

Fig. 2. Phase-plane trajectory of SNN (1) without control.

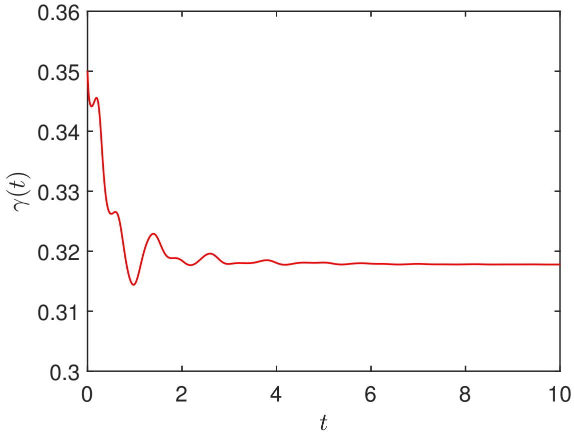

Fig. 4. Trajectory of $\gamma(t)$.

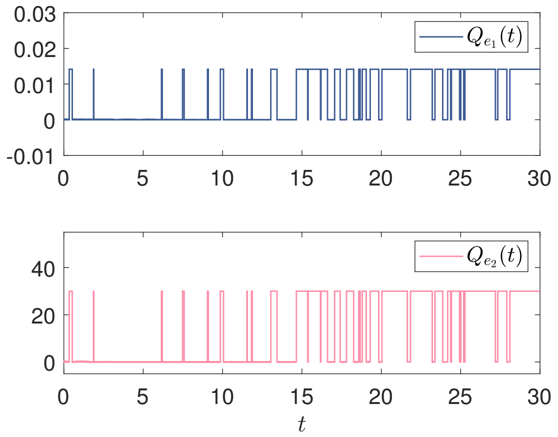

Fig. 3. Trajectories of $Q_{e_1}(t)$ and $Q_{e_2}(t)$.

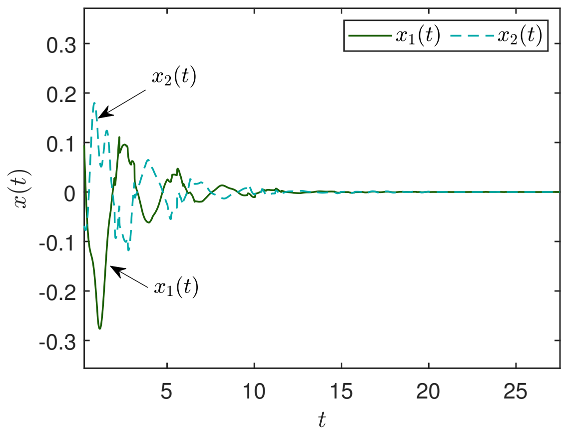

Fig. 5. State trajectories of the closed-loop SNN.

$$\mathcal{K}_{2,0} = \begin{bmatrix} 28.4558 & -11.2574 \\ -10.1306 & 29.8037 \end{bmatrix},$$

$$\mathcal{K}_{2,1} = \begin{bmatrix} 25.3922 & -14.4730 \\ -12.7879 & 26.6355 \end{bmatrix},$$

$$\mathcal{K}_{2,2} = \begin{bmatrix} 25.3877 & -14.4860 \\ -12.7908 & 26.6588 \end{bmatrix},$$

$$\mathcal{K}_{2,3} = \begin{bmatrix} 24.6422 & -14.8047 \\ -13.4990 & 26.3834 \end{bmatrix},$$

$$\mathcal{K}_{2,4} = \begin{bmatrix} 24.0152 & -15.0421 \\ -14.0861 & 26.1603 \end{bmatrix}.$$

When the initial condition is $x(s) = col\{0.4, -0.4\}$, Fig. 1 represents the phase-plane plot of Fig. 2 under the above switching signal without a control input, revealing the presence of the singular attractor.

Now we set initial condition $x(0) = col\{0.3, -0.3\}$. According to (5) and (24), we can know when $y(t) = 0$, $\psi_y(t) = 1$, when $y(t) \neq 0$,

$$\sqrt{0.0011}\|y(t)\| \leq \psi_y(t) \leq 2\sqrt{0.0011}\|y(t)\|,$$

then, the dynamic quantizer (4) can be derived as

$$Q(y(t)) = \begin{cases} 0, & y(t) = 0, \\ y(t) + \omega_q \psi_y(t) + sin(\frac{y(t)}{\psi_y(t)}), & y(t) \neq 0. \end{cases}$$

According to (8), we set

$$Q_{e_1}(t) = \sqrt{n_y}\psi_y(t)\omega_q - \|e_y(t)\|,$$
$$Q_{e_2}(t) = \psi_y(t)\omega_s - \|y(t)\|.$$

Then, the trajectories of $Q_{e_1}(t)$ and $Q_{e_2}(t)$, depicted in Fig. 3, remain non-negative, signifying the efficacy of the dynamic quantizer in preventing saturation.

In the condition of $x(h) = col\{0, 0\}$, $h \in [0, \nu)$, the trajectories of $\gamma(t)$ are drawn in Fig. 4, and the $\mathcal{L}_2$-gain formula designed in this article is as follows:

$$\gamma(t) = \sqrt{\int_0^t \|z(s)\|^2\, ds / \int_0^\infty \|w(s)\|^2\, ds},$$

this suggests that $\gamma(\infty) = 0.3178 (< \gamma^* = 0.7930)$. With the calculated feedback gains, the state trajectories of closed-loop SNN (12) are plotted in Fig. 5, showcasing rapid convergence.

From above, it can be seen that the system can still ensure the asymptotic stability of the system and maintain the $\mathcal{L}_2$-gain performance in the presence of faults, further illustrating the effectiveness of the feedback control scheme with dynamic output quantization given in this paper.

V. Conclusion

The problem of fault-tolerant quantized control for SNN (1) under PDT switching in the presence of actuator faults and dynamic output quantization was investigated. DSF $\psi_y(t)$ was constructed as a segmentation function, as shown in (5), to prevent the occurrence of division by zero of the output signal. To reduce conservatism, the controller is designed to combine the system model δ_t with a time scheduler r_t constructed with a minimum time span. A sufficient condition (see Theorem 1) for asymptotic stability and $\mathcal{L}_2$-gain in the closed-loop SNN is derived using a piecewise LKF (25) and decoupling methods. The needed feedback gains and the parameter range associated with the DSF can be determined by exact mathematical expressions (23) and (25) when the condition is satisfied. For comparison purposes, the feedback gains that depend only on the system mode δ_t are also studied, and the corresponding design method is proposed in Corollary 1. The numerical simulation results demonstrate the effectiveness of our proposed control scheme.

References

[1] L. Zhu, J. Qiu, and H. R. Karimi, "Region stabilization of switched neural networks with multiple modes and multiple equilibria: A pole assignment method," *IEEE Transactions on Neural Networks and Learning Systems*, vol. 31, no. 9, pp. 3280–3293, 2020.

[2] R. Vadivel, M. S. Ali, F. Alzahrani, J. Cao, and Y. H. Joo, "Synchronization of decentralized event-triggered uncertain switched neural networks with two additive time-varying delays," *Nonlinear Analysis: Modelling and Control*, vol. 25, no. 2, pp. 183–205, 2020.

[3] A. S. Morse, "Supervisory control of families of linear set-point controllers-part i. exact matching," *IEEE Transactions on Automatic Control*, vol. 41, no. 10, pp. 1413–1431, 1996.

[4] J. P. Hespanha and A. S. Morse, "Stability of switched systems with average dwell-time," in *Proceedings of the 38th IEEE Conference on Decision and Control*, vol. 3, Phoenix, AZ, USA, 1999, pp. 2655–2660.

[5] J. P. Hespanha, "Uniform stability of switched linear systems: Extensions of LaSalle's invariance principle," *IEEE Transactions on Automatic Control*, vol. 49, no. 4, pp. 470–482, 2004.

[6] L. Chen, Y. Tan, Y. Zhu, and H.-K. Lam, "Fault reconstruction for continuous-time switched nonlinear systems via adaptive fuzzy observer design," *IEEE Transactions on Fuzzy Systems*, vol. 31, no. 9, pp. 3235–3247, 2023.

[7] X. Song, Z. Peng, S. Song, and V. Stojanovic, "Anti-disturbance state estimation for PDT-switched RDNNs utilizing time-sampling and space-splitting measurements," *Communications in Nonlinear Science and Numerical Simulation*, vol. 132, p. 107945, 2024.

[8] C. Wei, X. Xie, J. Sun, and J. H. Park, "Attack-resilient dynamic-memory event-triggered control for fuzzy switched systems with persistent dwell-time," *IEEE Transactions on Fuzzy Systems*, vol. 32, no. 5, pp. 3154–3164, 2024.

[9] A. Banerjee, S. M. Amrr, R. Sarkar, A. S. Saidi, and M. Nabi, "Communication constrained robust guidance strategy using quantized artificial time delay based control with input saturation," *IET Control Theory & Applications*, vol. 15, no. 18, pp. 2286–2301, 2021.

[10] T.-F. Li, X.-H. Chang, and J. H. Park, "Quantized-output-based exponential stabilization of fuzzy DPSs with time-varying delay and nonlinearities," *IEEE Transactions on Fuzzy Systems*, vol. 31, no. 7, pp. 2360–2374, 2023.

[11] J. Dong, X. Ma, X. Zhang, J. Zhou, and Z. Wang, "Finite-time $\mathcal{H}_\infty$ filtering for Markov jump systems with uniform quantization," *Chinese Physics B*, vol. 32, no. 11, p. 110202, 2023.

[12] C. Guan, Z. Fei, H. R. Karimi, and P. Shi, "Finite-time synchronization for switched neural networks via quantized feedback control," *IEEE Transactions on Systems, Man, and Cybernetics: Systems*, vol. 51, no. 5, pp. 2873–2884, 2021.

[13] F. Liu, Y. Yang, F. Wang, and L. Zhang, "Synchronization of fractional-order reaction–diffusion neural networks with Markov parameter jumping: Asynchronous boundary quantization control," *Chaos, Solitons & Fractals*, vol. 173, p. 113622, 2023.

[14] Z. Yan, D. Zuo, T. Guo, and J. Zhou, "Quantized $\mathcal{H}_\infty$ stabilization for delayed memristive neural networks," *Neural Computing and Applications*, vol. 35, no. 22, pp. 16 473–16 486, 2023.

[15] R. Saravanakumar, A. Amini, R. Datta, and Y. Cao, "Reliable memory sampled-data consensus of multi-agent systems with nonlinear actuator faults," *IEEE Transactions on Circuits and Systems II: Express Briefs*, vol. 69, no. 4, pp. 2201–2205, 2022.

[16] Z. Wen, X. Bie, and S. Tan, "Neuroadaptive fixed-time tracking control of full-state constrained strict-feedback nonlinear systems with actuator faults." *Engineering Letters*, vol. 32, no. 3, pp. 503–511, 2024.

[17] X. Jin, X. Zhao, J. Yu, X. Wu, and J. Chi, "Adaptive fault-tolerant consensus for a class of leader-following systems using neural network learning strategy," *Neural Networks*, vol. 121, pp. 474–483, 2020.

[18] G. Zhang, S. Chu, X. Jin, and W. Zhang, "Composite neural learning fault-tolerant control for underactuated vehicles with event-triggered input," *IEEE Transactions on Cybernetics*, vol. 51, no. 5, pp. 2327–2338, 2021.

[19] M. Wang, S. Zhu, M. Shen, X. Liu, and S. Wen, "Fault-tolerant synchronization for memristive neural networks with multiple actuator failures," *IEEE Transactions on Cybernetics*, pp. 1–10, 2024.

[20] W. Tai, X. Li, J. Zhou, and S. Arik, "Asynchronous dissipative stabilization for stochastic Markov-switching neural networks with completely-and incompletely-known transition rates," *Neural Networks*, vol. 161, pp. 55–64, 2023.

[21] Y. Wang and Z. Yan, "Adaptive synchronization for inertial cohen-grossberg neural networks with distributed delay." *Engineering Letters*, vol. 31, no. 4, pp. 1486–1491, 2023.

[22] M. Sathishkumar and Y.-C. Liu, "Hybrid-triggered reliable dissipative control for singular networked cascade control systems with cyber-attacks," *Journal of the Franklin Institute*, vol. 357, no. 7, pp. 4008–4033, 2020.

[23] X. Wang, Y. Wang, and W. Hou, "Event-based reliable control for switched systems with actuator failures and nonlinear perturbation," *IAENG International Journal of Computer Science*, vol. 48, no. 3, pp. 463–470, 2021.

[24] J. Zhou, J. Dong, and S. Xu, "Asynchronous dissipative control of discrete-time fuzzy Markov jump systems with dynamic state and input quantization," *IEEE Transactions on Fuzzy Systems*, vol. 31, no. 11, pp. 3906–3920, 2023.

[25] Y. Chen, X. Zhang, Z. Yan, O. Faydasicok, and S. Arik, "Sampled-data control for markovian switching neural networks with output quantization and packet dropouts," *Journal of the Franklin Institute*, vol. 361, no. 18, p. 107252, 2024.

[26] L. Xie, M. Fu, and C. E. de Souza, "$\mathcal{H}_\infty$ control and quadratic stabilization of systems with parameter uncertainty via output feedback," *IEEE Transactions on Automatic Control*, vol. 37, no. 8, pp. 1253–1256, 1992.

[27] J. Zhou, X. Ma, Z. Yan, and S. Arik, "Non-fragile output-feedback control for time-delay neural networks with persistent dwell time switching: A system mode and time scheduler dual-dependent design," *Neural Networks*, vol. 169, pp. 733–743, 2024.

[28] G. Chen, J. Xia, J. H. Park, H. Shen, and G. Zhuang, "Sampled-data synchronization of stochastic Markovian jump neural networks with time-varying delay," *IEEE Transactions on Neural Networks and Learning Systems*, vol. 33, no. 8, pp. 3829–3841, 2022.

[29] S. Dong and M. Liu, "Adaptive fuzzy asynchronous control for nonhomogeneous Markov jump power systems under hybrid attacks," *IEEE Transactions on Fuzzy Systems*, vol. 31, no. 3, pp. 1009–1019, 2023.

[30] Y. Wang, “Stabilization and $\mathcal{L}_2$-gain for a class of switched systems with nonlinear disturbance and time-varying delay,” *IAENG International Journal of Applied Mathematics*, vol. 49, no. 1, pp. 98–108, 2019.

[31] H. Lu, “Chaotic attractors in delayed neural networks,” *Physics Letters A*, vol. 298, no. 2-3, pp. 109–116, 2002.